IEEE Robotics and Automation Letters (RA-L) paper, presented at ICRA 2026, Vienna, Austria. Cite as RA-L paper.

Stability Analysis of a Dual-Rate Haptic System: A New Closed-Form Solution

Ahmad Mashayekhi, Oumaima Akhif, Amin Khorasani, and Tom Verstraten, *Member, IEEE*

***Abstract*—Haptic devices (HDs) play a vital role in simulating the sense of touch in various virtual environments (VEs). Ensuring stable interaction between the HD and the VE is critical, particularly when simulating stiff virtual objects. One approach to enhancing stability is increasing the sampling rate; however, excessively high rates can compromise velocity information, thereby reducing damping stability. Dual-rate haptic devices address this issue by sampling position at higher rates and velocity at lower rates. This paper presents a novel closed-form equation for predicting the stability boundary of a dual-rate HD without restrictions on time delay or virtual damping. The proposed equation, which depends on the physical parameters of the HD and VE, sampling times, and time delay, is validated through simulations and experiments.**

***Index Terms*—Dual-rate, haptic device, stability, time delay.**

I. Introduction

HAPTIC devices (HDs) transmit forces from virtual environments (VEs) to human operators. Their applications include teleoperation simulators [1], haptic guidance [2], and human-robot interaction [3]. To ensure effective performance, HDs should have minimal mass, inertia, and friction, making their dynamics negligible compared to those of the VE.

When interacting with a real object, the contact force can be modeled using a spring and a damper. Similarly, the virtual environment is modeled as a discrete spring with stiffness K and a damper with damping coefficient B. Position data is used to calculate velocity through the backward difference method, enabling the simulation of virtual damping.

Haptic devices (HDs) are often multi-DOF manipulators, typically simplified to a 1-DOF system when simulating a virtual environment (VE) for an operator. In this simplification, the HD's dynamics are represented by an effective mass with viscous and Coulomb friction, and its position is measured with an effective sensor resolution, which indicates the smallest detectable displacement [4], [5] in movement direction. This approach has been widely used in stability and passivity analyses [6], [7], [8], [9].

Received 23 November 2024; accepted 13 April 2025. Date of publication 9 May 2025; date of current version 19 May 2025. This article was recommended for publication by Associate Editor K. Hashtrudi-Zaad and Editor J.-H. Ryu upon evaluation of the reviewers' comments. This work was supported by the Research Foundation Flanders (FWO) SBO-ELYSA Project under Grant S001821N. *(Corresponding author: Ahmad Mashayekhi.)*

Ahmad Mashayekhi, Amin Khorasani, and Tom Verstraten are with the Brubotics, Vrije Universiteit Brussel, 1050 Brussels, Belgium, and also with the Flanders Make, 1000 Brussels, Belgium (e-mail: ahmad.mashayekhi@vub.be).

Oumaima Akhif is with the Brubotics, Vrije Universiteit Brussel, 1050 Brussels, Belgium.

Digital Object Identifier 10.1109/LRA.2025.3568643

Increasing the maximum renderable value of K is a key focus of research in haptic rendering. One way to achieve this is by using faster sampling rates to read sensor data and calculate velocity using the backward difference method, as demonstrated in various studies (e.g., [6]). However, excessively high sampling rates can lead to inaccurate velocity estimation, making the HD unstable [10]. This issue worsens with higher sampling rates, lower sensor resolution, or when calculating acceleration from the velocity signal, which is essential for simulating virtual mass applications [11], [12], [13].

Using more precise sensors can reduce the resulting error in velocity estimation, but this solution can be costly. Another option is applying a velocity filter or using adaptive windowing for velocity estimation. Instead of computing velocity using the backward difference method, this approach calculates the difference over multiple previous steps. As a result, velocity is determined at a slower rate, but the viscous force is updated more frequently—once per sampling period [14], [15].

An alternative approach to address this issue is by using two different sampling rates for reading position and calculating velocity. Specifically, a higher sampling rate is used to read the sensor position, which is then used in the required control loop, while a lower sampling rate is employed to calculate velocity in order to avoid noise and inaccurate estimation. This type of system is called a *dual-rate* (haptic) system. This concept has been applied in control systems, as in [16], as well as in haptic systems, such as [17].

The novelty of this paper lies in presenting an analytical stability analysis of a dual-rate HD, resulting in a new set of closed-form equations that can predict the stability boundary of the dual-rate HD as a function of the physical parameters of the HD and VE, sampling times, and time delays. The key contribution is that these new closed-form equations are valid for both small and large values of virtual damping and time delays. Based on these equations, the entire stability boundary can be determined directly (i.e., without the need for any iteration), quickly and precisely.

The structure of this paper is as follows. Section II begins with a review of previous analyses, followed by Section III, which presents the modeling and stability analysis of the dual-rate HD. Simulations and experiments are presented in Section IV to verify the theoretical results. The obtained results are discussed and compared with the existing literature in Section V. The paper concludes in Section VI with conclusions and future work, and finally ends with the references in Section VI.

IEEE Robotics and Automation Letters (RA-L) paper, presented at ICRA 2026, Vienna, Austria. Cite as RA-L paper.

II. Prior Work

The stability of single-rate haptic systems was first studied by modeling the HD as a continuous linear system with a mass of m and viscous friction of b [18]. The VE was modeled as a virtual stiffness of K, and a time delay of one sampling time was considered in the control loop (i.e., $t_d = T$). In this analysis, the effect of operator dynamics was neglected—an approach commonly referred to as *uncoupled stability*. In many subsequent studies, the backward difference method was also used for discretization. These two assumptions are widely adopted in the literature and are also used in the theory presented in this paper. The result was the following theoretical stability boundary equation:

$$K = \frac{b}{T}. \tag{1}$$

Further studies in this field have confirmed this factor of two through theoretical approaches [10]. Stability analysis of a 1-DOF single-rate HD with mass and viscous friction, while modeling the VE as a digital spring (K) and damper (B) without time delay, was conducted in [7], leading to the following stability equation:

$$K = \frac{2(B+b)}{T}. \tag{2}$$

The above equation is valid only for small values of the virtual damping (B). When considering a time delay of t_d in the control of the HD, the following stability equation is determined [8]:

$$K = \frac{B+b}{T/2+t_d}. \tag{3}$$

It should be noted that both (2) and (3) are valid for small values of B and t_d. Whereas, in the case of no time delay (i. e. $t_d = 0$), the stability boundaries for large values of virtual damping were plotted, and the entire stability region was determined in [7], [8], [11].

The stability, passivity, and fidelity of haptic simulation systems using a generalized discretization method, considering dimensionless parametrization and rational delay for device-independent analysis is analyzed in [19].

A closed-form stability equation is presented in [20] that can predict the entire stability boundary without any limitations on B or t_d, as follows:

$$\begin{cases} K = T\omega^2 \frac{m\omega\cos((T+t_d)\omega) + b\sin((T+t_d)\omega)}{\sin(T\omega)} \\ B = T\omega \frac{m\omega\sin((T/2+t_d)\omega) - b\cos((T/2+t_d)\omega)}{\sin(T\omega)}, \end{cases} \tag{4}$$

where ω is the frequency, which varies from zero to a maximum value of $\omega_{\max}$ that makes the numerator of K equal to zero. The nonzero answer for $\omega_{\max}$ is determined as follows [20]:

$$\omega_{\max} = \frac{1}{T+t_d}.\frac{-(p_2 - aq_1) - \sqrt{(p_2 - aq_1)^2 - 4p_3(p_1 - a)}}{2(p_1 - a)} \tag{5}$$

In this equation, $a = m/b(T+t_d)$ and $p_1 = -0.4087$, $p_2 = 1.325$, $p_3 = 0.07507$ and $q_1 = -\pi/2$ [20].

Using this pair of equations, the stability boundaries can be determined quickly and with good precision, without any limitations on time delay or virtual damping. This method is extended in the current paper to determine the new stability boundaries for the dual-rate haptic system.

Dual-rate control for motion control applications is a concept used in research such as [16] to improve performance. Dual-rate control in haptic systems was introduced in [21] to extend the stable range of the control system, particularly for virtual models that were simulated slowly. It was demonstrated that the energy produced by the traditional controller could be balanced by the additional high-frequency controller. This was shown through experiments and the development of stability inequality equations. By adding the high-frequency controller and accounting for user dynamics, the stiffness was increased by 1.5 times.

Subsequently, in [22], it was demonstrated that this dual-rate control technique can increase the maximum virtual stiffness, particularly for the stability of a haptic dental training system. This was shown experimentally, taking into account the dynamics of the user, as well as computationally using inequality equations.

As recommended in [23], improving velocity estimation requires sophisticated techniques such as the Kalman filter, first-order adaptive windowing, and low-pass filtering. However, these techniques increase the time required to calculate velocity, which could raise the total delay and reduce the stable zone.

The idea of dual-rate sampling for haptic interfaces to expand the stability region of the HD is introduced in [24]. The traditional single-rate controller is modified by sampling the position and velocity loops at different rates, rather than incorporating a high-frequency controller. They proposed using two different sampling rates: one for reading position and another for calculating velocity. However, they did not account for time delay, and no closed-form equation was provided for estimating the stability boundary. Additionally, the following equation is derived for small virtual damping values:

$$K = \frac{2(B+b)}{T/N}, \tag{6}$$

where T and T/N are the sampling times for calculating velocity and reading position, respectively.

The discrete-time root-locus method is used to perform a theoretical stability analysis of a dual-rate haptic system [25]. For two distinct configurations, the boundaries of virtual damping and stiffness were determined iteratively as a function of the ratio between the sampling times. In the first setup, the sampling period of the velocity loop remained constant, while the sampling period of the position loop was shortened. In the second setup, the sampling period of the velocity loop was extended, while the sampling period of the position loop remained fixed.

Later, time delay was also taken into account [26]. Using the precise discrete-time approach, stability boundaries were identified. However, since the system's order depends on the sampling rate and the magnitude of the time delay, these analyses are computationally intensive, particularly for large time delays. To reduce the high dimensionality, slow-fast model decomposition was explored for model order reduction [27]. Additionally, the equivalent continuous-time technique, which is only applicable for small time delays, was used to obtain less conservative stability boundaries. By employing various transformations through

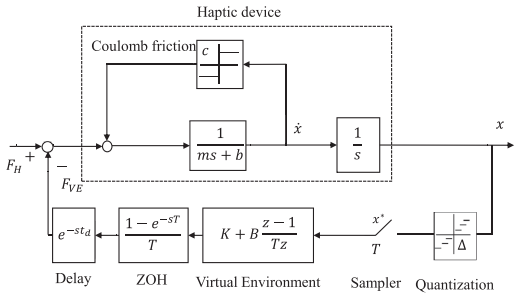

Fig. 1. The nonlinear model of a single-rate haptic device.

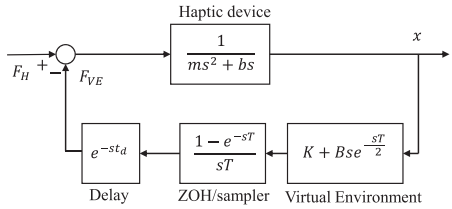

Fig. 2. The linear model of a single-rate haptic device.

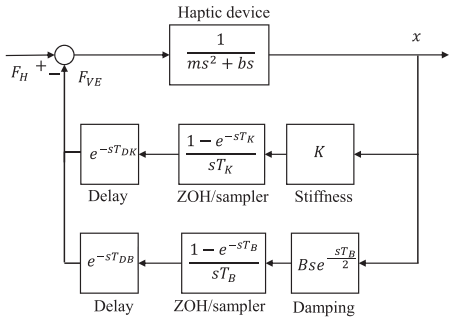

Fig. 3. Schematic diagram of a dual-rate haptic device.

discrete-time root locus methods, it became possible to derive a discrete-time root locus as a function of either K or B.

Recently, Ganiny et al. extended stability analyses to multi-DoF dual-rate haptic systems [28]. Their study formulated the coupled dynamics of a multi-DoF haptic device with a dual-rate sampling system and analyzed its stability using a discrete-time state-space approach with dynamic decoupling. It examined the effects of time delay, mechanical design, and dual-rate sampling on stability across the workspace. Additionally, a model-order reduction (MOR) framework was employed to simplify stability limit determination, independent of time delay and sampling rate variations. Using this MOR framework, the stability boundaries can be determined through a few iterations. It will be shown that the stability equations presented in this paper are significantly faster than even the MOR framework.

Based on the reviewed literature, closed-form stability equations exist for single-rate haptic systems that can predict the stability boundary of the HD without any limitations on time delay and virtual damping. However, such equations do not exist for dual-rate haptic systems. Therefore, this paper addresses this gap, and the results are verified through simulations and experiments.

III. Modeling and Stability Analysis

A. Modeling

The effect of a human operator's hand on stability analysis has been studied in various works, showing that it can improve the stability boundary of the haptic system [8], [29]. Thus, while studying the stability or passivity of HDs, the effect of the operator's hand is often neglected.

Based on the results of [4], [5], we assume that the nonlinear dynamics of the HD can be simplified to a 1-DOF mass m, with viscous friction b and Coulomb friction c. Its output is sensed by a sensor with limited resolution, and after sampling, the sampling time T is used in the VE model (as shown in Fig. 1). Since most real objects can be simulated by spring and damper elements, the VE is assumed to be a discrete spring-damper model. The force/torque from the VE passes through a zero-order hold block (ZOH) and a time delay of t_d. In Fig. 1, two nonlinear phenomena are depicted: Coulomb friction and sensor quantization. The former dissipates energy during motion, while the latter may introduce energy into the haptic system. Studies such as [30], [31] have shown that the maximum energy introduced by quantization is always less than the energy dissipated by Coulomb friction in most commercial HDs. Therefore, these two nonlinear phenomena are omitted from the haptic model to facilitate stability and passivity analyses such as those in [7], [8], [9], [32] (as depicted in Fig. 2).

In Fig. 2, a continuous model of the VE is presented, which has been previously used in [6], [20], [29]. Additionally, the sampler and zero-order hold are combined, and the time delay is represented in its continuous form.

In the case of using two different sampling rates for position and velocity, the HD model will be modified as depicted in Fig. 3. In this figure, two feedback loops exist. One feedback loop relates the stiffness of the VE (K) with the sampling time of T_K and the time delay of T_{DK}. The other one calculates the velocity with the sampling time of T_B and relates the damping (B) with the time delay of T_{DB}. This figure will be used for the determination of the new stability equations.

B. Stability Analysis

Here it is assumed that the existence of a dual-rate HD that utilizes appropriate sampling rates to mitigate the noise and uncertainty in velocity calculation, and based on this assumption, the stability analysis is performed. To study the stability of the dual-rate HD shown in Fig. 3, the closed-loop transfer function of the system is first derived as shown in (7):

$$G_c(s) = \frac{sT_KT_B}{d(s)}, \tag{7}$$

where its denominator is the characteristic equation:

$$d(s) = (ms^2+bs)sT_KT_B + Ke^{-sT_{DK}}\left(1-e^{-sT_K}\right)T_B + Bse^{-sT_B/2}\,e^{-sT_{DB}}\left(1-e^{-sT_K}\right)T_K \tag{8}$$

The roots of the characteristic equation correspond to the poles of the closed-loop transfer function. All of the transfer function's

IEEE Robotics and Automation Letters (RA-L) paper, presented at ICRA 2026, Vienna, Austria. Cite as RA-L paper.

poles must lie in the left half-plane for stability. When a pole is purely imaginary (i.e., $s = j\omega$), the boundary of stability is reached. By substituting $s = j\omega$ and $e^{j\omega} = \cos(\omega) + j\ \sin(\omega)$ into the characteristic equation, it simplifies to $R + jI = 0$, where R and I represent the real and imaginary parts of the characteristic equation, as shown in (9) and (10) shown at the bottom of this page, respectively.

By solving $R = 0$ and $I = 0$ for K and B, and after simplification, the following equations are obtained:

$$\begin{cases} K = T_K\omega^2 \frac{m\omega cos(\omega(T_B+T_{DB}))+bsin(\omega(T_B+T_{DB}))}{2sin\left(\frac{\omega T_K}{2}\right)cos\left(\omega\left(\frac{T_K}{2}+T_{DK}-T_B-T_{DB}\right)\right)} \\ B = T_B\omega \frac{\omega msin(\omega(T_K/2+T_{DK}))-bcos(\omega(T_K/2+T_{DK}))}{2sin\left(\frac{\omega T_B}{2}\right)cos\left(\omega\left(\frac{T_K}{2}+T_{DK}-T_B-T_{DB}\right)\right)} \end{cases} \tag{11}$$

In this pair of equations, ω represents the frequency, which ranges from zero to a maximum value that results in $K = 0$. By comparing the K of this equation with K in the case of the single-rate HD (i.e. (4)), it is found that to obtain the nonzero value of $\omega_{\max}$, T and t_d should be replaced by T_B and T_{DB} in (5), respectively, as follows:

$$\omega_{\max} = \frac{1}{T_B + T_{DB}} \cdot \frac{-(p_2 - aq_1) - \sqrt{(p_2 - aq_1)^2 - 4p_3(p_1 - a)}}{2(p_1 - a)}. \tag{12}$$

In this equation, $a = \frac{m}{b(T_B+T_{DB})}$, and the constants are $p_1 = -0.4087$, $p_2 = 1.325$, $p_3 = 0.07507$, and $q_1 = -\pi/2$.

Using these new equations, the stability boundaries of a dual-rate haptic system can be determined quickly and easily, without any limitations on time delays or virtual damping. These equations will be verified through simulations and experiments in the following sections. It should be noted that when using a rotary HD, the inertia value should be used instead of m. In this case, b represents the rotary viscous damping, while K and B correspond to the rotary system with appropriate SI units.

The need for real-time determination of stability boundaries arises in several situations. For example, when using a multi-DOF haptic device (HD), such as a phantom desktop HD with 6-DOF, the effective mass and viscous friction values change significantly depending on the location and orientation of the HD's stylus [5] and [4]. These variations, in turn, affect the stability boundaries and the z-width of the HD. By using the presented closed-form stability equations, the entire stability boundary can be determined very quickly—more than 10^5 times faster than the reduced-order method. Another application is when the simulated environment parameters are estimated online rather than known beforehand. In such cases, while rendering a virtual environment, it is essential to ensure that the required stiffness is renderable. If necessary, additional virtual damping or virtual mass can be introduced to maintain stability, as suggested in [33] and [20].

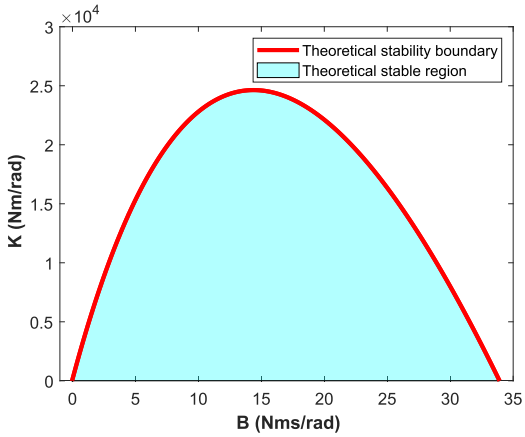

Fig. 4. Typical stability boundary of a dual-rate haptic system plotted by (11), for the mentioned parameters.

A typical stability boundary with sampling times of $T_K = 0.1$ ms and $T_B = 0.2$ ms, time delays of $T_{DK} = 0.2$ ms and $T_{DB} = 0.4$ ms, and physical parameters of $m = 0.0128$ kg.m^2 and $b = 0.0324$ Nms/rad (according to the physical parameters of the experimental setup) is plotted as shown in Fig. 4. The solid red line represents the stability boundary. Operating points below this curve will result in stable operation, while points above the curve will lead to unstable behavior.

The starting point of the stability curve corresponds to $\omega = 0$. Using limit techniques, it can be shown that, regardless of the physical parameters of the HD, sampling times, and time delays, the stability curves always begin at $(B, K) = (-b, 0)$. This finding is consistent with the results of [22] and [24] for dual-rate HDs.

It can be shown that, when using the same sampling times and time delays (i.e., $T_K = T_B = T$ and $T_{DK} = T_{DB} = t_d$), the dual-rate stability equations from (11) simplify directly to the single-rate stability equations of (4). In this case, with the additional assumption of small values for the virtual damping and time delay, the new stability equations are simplified to (3).

IV. Validation

In this section, the stability equations determined in (11) are verified through simulations and experiments.

$$\begin{aligned} R = {} & KT_B\left[\sin(T_K\omega)\sin(\omega T_{DK}) - \cos(\omega T_{DK})(\cos(T_K\omega) - 1)\right] \\ & - BT_K\omega\left[\sin\left(\frac{\omega}{2}(3T_B + 2T_{DB})\right) - \sin\left(\frac{\omega}{2}(T_B + 2T_{DB})\right)\right] - T_BT_K\omega^2 b \end{aligned} \tag{9}$$

$$\begin{aligned} I = {} & KT_B\left[\sin(T_K\omega)\cos(\omega T_{DK}) + \sin(\omega T_{DK})(\cos(T_K\omega) - 1)\right] \\ & - BT_K\omega\left[\cos\left(\frac{\omega}{2}(3T_B + 2T_{DB})\right) - \cos\left(\frac{\omega}{2}(T_B + 2T_{DB})\right)\right] - T_BT_K\omega^3 m \end{aligned} \tag{10}$$

IEEE Robotics and Automation Letters (RA-L) paper, presented at ICRA 2026, Vienna, Austria. Cite as RA-L paper.

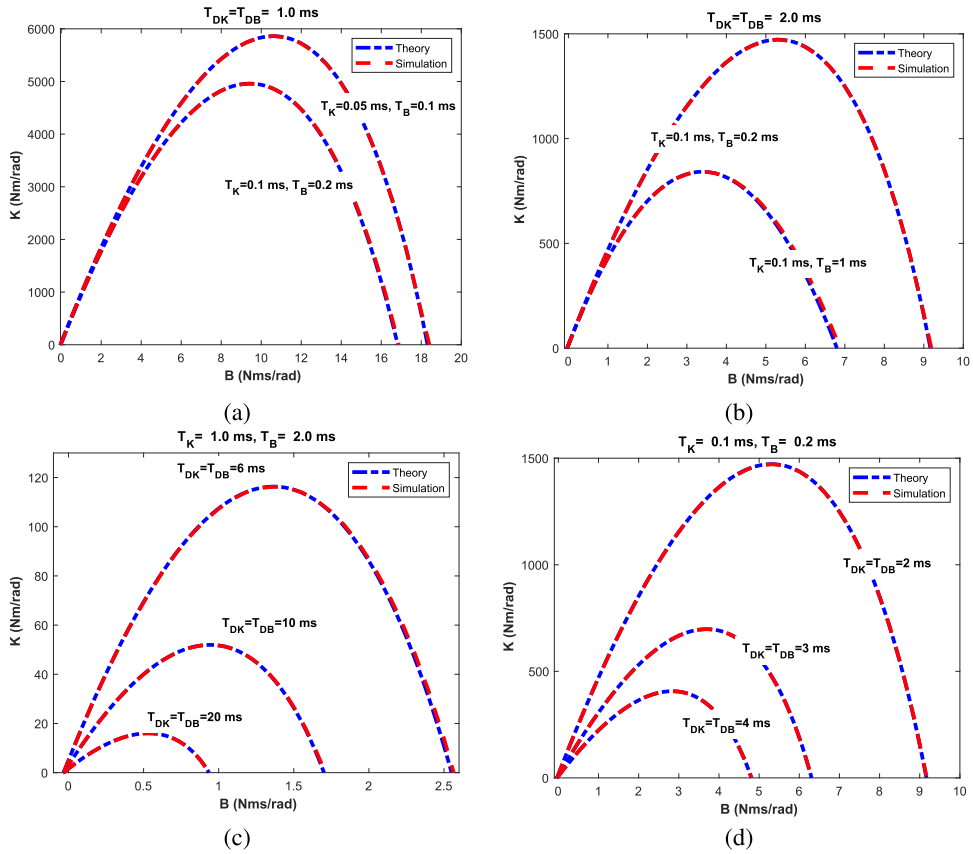

Fig. 5. The theoretical stability boundaries (dash-dotted blue lines, determined from (11)) are compared to the stability regions determined by simulations (dashed red lines) for different values of sampling times and time delays.

A. Simulations

In this section, the theoretical stability boundaries (derived from (11)) are compared with the stability boundaries obtained from a series of simulations using MATLAB Simulink. For this purpose, a rotary haptic device with physical parameters of 0.0128 kg.m^2 and 0.0324 Nms/rad (according to the physical parameters of the experimental setup) is selected. The VE is modeled as a discrete spring-damper system, while various values of sampling times and time delays are considered, along with zero-order hold blocks. The theoretical stability boundaries are plotted using (11), and the simulation results are obtained by iteratively adjusting K through a bisection search method, based on the stability behavior of the system, to determine the maximum achievable value of K for stable interactions. The result is shown in Fig. 5. From this figure, it can be concluded that the theoretical equations presented here accurately predict the stability boundary for different combinations of time delays and sampling times.

B. Experiments

As mentioned in the Introduction, using a single-rate control system with a very high sampling rate (e.g., 10 or 20 kHz) leads to noisy velocity estimation, which negatively impacts the maximum renderable stiffness. This phenomenon has been experimentally observed in many previous studies across various fields (e.g., [10], [23], [24]). Therefore, this paper does not aim to repeat experiments to demonstrate this effect again. Instead, it focuses on validating the theoretically established stability equations through experiments.

A dual-motor actuator (DMA) consists of two motors coupled through a planetary differential. These two independent motors rotate the sun and the ring of the planetary gearbox, while the carrier of the planetary gearbox is considered the output [34].

Locking the ring, effectively making it equivalent to a regular drivetrain consisting of a motor *(Maxon ECi-52)* and planetary gearbox, is used as a 1-DOF experimental haptic setup in this paper.

The paddle side of this haptic device has an inertia of 0.0128 kgm^2 and viscous friction of 0.0324 Nms/rad [35]. The inertia of the paddle side of the HD was determined using the CAD model and the mechanical properties of each component, based on known material characteristics. The calculated inertia was then reflected at the system's output, accounting for the gear ratio. To estimate viscous friction, a simple identification procedure was performed by observing the system's free motion without any interaction with the environment. The recorded torque during motion was then fitted using Coulomb and viscous friction models to determine the friction parameters.

A 3-channel incremental encoder with 4096 pulses per revolution is used to measure the angle of the paddle. The resolution is enhanced through a gear train and sensor quadrature, effectively

IEEE Robotics and Automation Letters (RA-L) paper, presented at ICRA 2026, Vienna, Austria. Cite as RA-L paper.

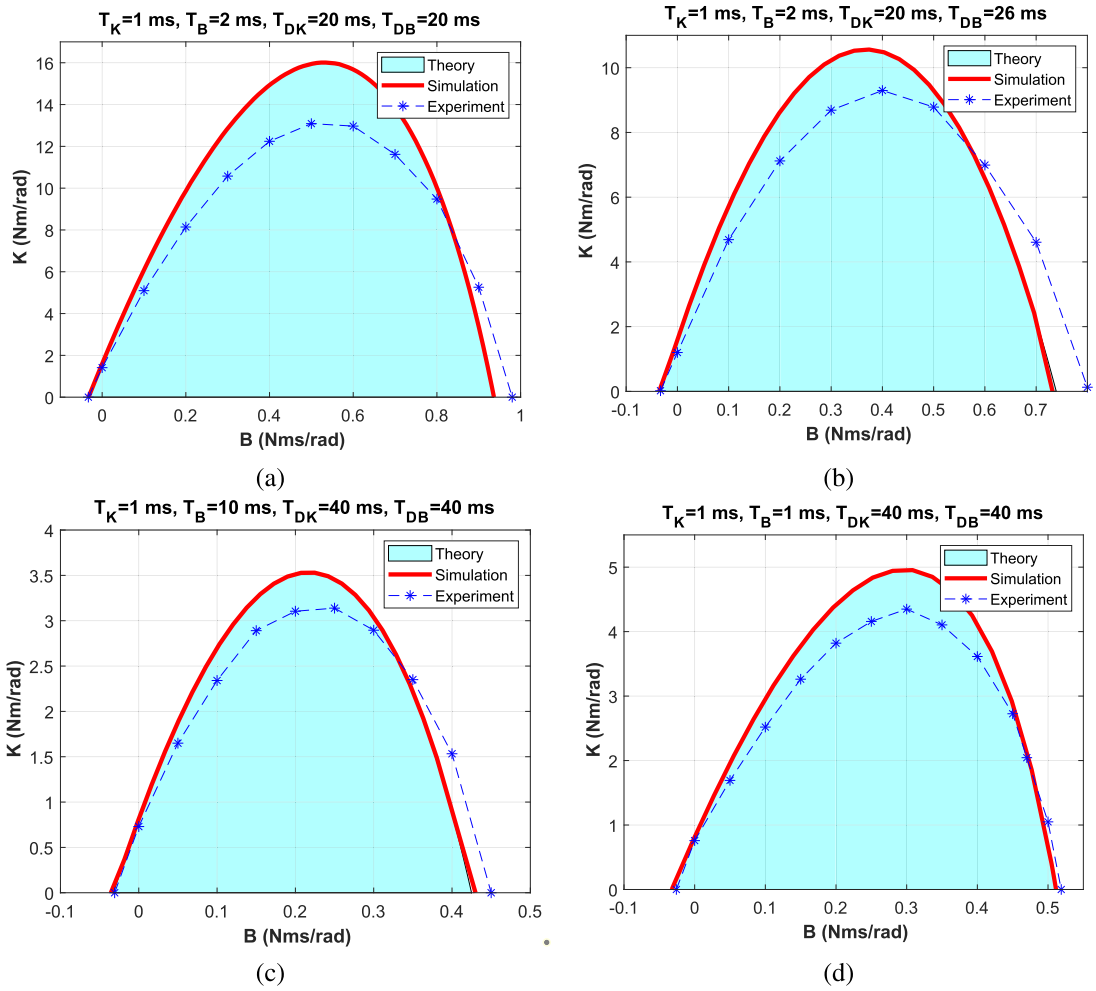

Fig. 6. The theoretical stability boundaries (red solid lines, determined from (11)), the stability regions determined by simulations (highlighted areas), and the experimental stability boundaries (blue dashed line with stars), for the different mentioned values of the sampling times and time delays.

increasing the measurement precision. As a result, the final angular resolution of the system is approximately 3 arc-seconds, ensuring accurate tracking of the paddle's motion. Gravitational torque and Coulomb friction are compensated by an internal controller.

The desired torque was commanded to the Sun motor by a Maxon EPOS4 70/15 driver. To avoid high values of K and severe vibrations, time delays were chosen such that the maximum renderable stiffness was limited. Due to limitations of the electrical equipment for real-time communication between the HD and the PC, the fastest achievable sampling rate was 1 ms. During the experiments, different sampling times and time delays were set and used. The theoretical stability boundary, determined from (11), was verified by both simulations and experiments through the trial-and-error method mentioned in the previous section, as depicted in Fig. 6.

V. Discussion

From Fig. 6, it can be seen that for all four different values of the sampling times and time delays, the theoretical stability boundaries (shaded areas) align well with the simulation results (red solid lines). However, there are some slight differences between the theoretical and experimental results (blue dashed lines with stars). A closer inspection of Fig. 6(d) provides an explanation for this slight difference. The haptic system studied in this figure has $T_K = T_B = 1$ ms and $T_{DK} = T_{DB} = 40$ ms, meaning the dual-rate HD is effectively turned into a single-rate HD. The stability analysis of this system was reported in prior works, e.g., [6], [20], [29], and it is shown to have very good accuracy in predicting the stability boundaries of the HD. Thus, the difference between the experimental results and theory exists even in the single-rate HD, possibly due to different sources of sensor quantization, internal controllers inside motor drivers, motor saturation, and limited accuracy in parameter identification of the HD.

As mentioned earlier, both the theoretical and experimental analyses assume that the sampling rates are not excessively high, and that velocity calculation noise is negligible. This assumption was also used in [26] when performing stability analysis using the discrete-time approach or the model-order reduction method. In this case, increasing the sampling time introduces greater time delays into the system, which can lead to instability in the HD. This is illustrated in Fig. 6(c) and (d): since velocity estimation

IEEE Robotics and Automation Letters (RA-L) paper, presented at ICRA 2026, Vienna, Austria. Cite as RA-L paper.

noise is absent in both figures, a lower sampling time results in a larger stability boundary. Furthermore, in all cases, including the other figures, the experiments validate the determined stability boundaries.

The reduced-order model approximates the original higher-order model, as published in [26]. However, both models share the same stability properties. This is achieved by applying the model order reduction technique to the closed-loop state-space model of the time-delayed dual-rate HD. For this purpose, a variety of stable and unstable time delay and sampling rate combinations were selected to determine the expected order of the reduced-order model. Based on these empirical observations, the dual-rate HD can be represented by a third-order reduced model for stability analysis in the most common time delay and sampling rate combinations. This implies that determining the order of the reduced model requires simulations and added effort. In contrast, deriving the closed-form stability equations of (11) is straightforward and can be done easily. The situation becomes even more complex when introducing a new linear block (e.g., a velocity filter, actuator dynamics, or operator hand dynamics) into the dual-rate HD model. In such cases, it should be examined whether the third-order model remains sufficient or if a higher-order model is required. In [20], [29], continuous-time stability analysis was performed, demonstrating that any linear block can be added to the system while still determining its effect on the stability boundary. For example, the impact of a low-pass filter was studied in [20], while the effect of the operator's hand was analyzed in [29].

The new closed-form stability equations presented in this paper significantly reduce computational time compared to the method used in [26] for determining stability boundaries. As reported in [26], stability boundaries were determined by gradually increasing B and iteratively searching for the maximum stable K using a discrete-time Lyapunov equation, requiring multiple iterations. In contrast, the proposed closed-form equations allow the entire stability boundary to be plotted without iterations, making the process much faster.

Computational time comparisons highlight this advantage: while the reduced-order model in [26] required 0.030 seconds to compute a single pair of (B, K) on the stability boundary, our method determined 10^6 pairs of (B, K) in under 0.1 seconds—computing each pair in less than 10^{-7} seconds, which is substantially faster than the reduced-order model. This demonstrates the significant advantage of using closed-form equations over iterative numerical methods for stability analysis.

This benefit was utilized in our experiments. Specifically, the low computational time of the entire stability boundaries allowed us to determine suitable values for the time delays and sampling times, ensuring that our experimental setup could implement them. For example, empirical observations indicate that rendering stiffness greater than $100\ \mathrm{Nm/rad}$ leads to actuator saturation and severe vibrations. Additionally, the maximum value of B is quickly determined and can be divided into the required intervals, allowing the maximum of K to be found at each point of B.

Model order reduction simplifies the determination of stability boundaries for the dual-rate HD, but reduced-order models remain approximations and require validation before use in system identification [26]. In contrast, the proposed closed-form stability equations can be directly applied to system identification, as demonstrated in [36] using stability boundaries from [20], [29]. Since these equations are derived from [20], they can also be utilized for identification.

Another advantage of using closed-form equations is the ease with which the effect of each parameter on the stability boundaries can be explored. For instance, the effect of parameter changes can be analyzed by partially differentiating K and B with respect to the parameter. As demonstrated in [20], the maximum renderable stiffness for large time delays was determined using this differentiation method.

VI. Conclusion and Future Work

In this brief, a new stability analysis of a dual-rate haptic system was conducted. A fast sampling rate is used for reading position and calculating the force of the virtual spring to increase the maximum renderable stiffness. A lower sampling rate is used for calculating velocity via the backward difference method, ensuring that uncertainties in velocity calculation are minimized. This dual-rate control system can lead to rendering larger values of virtual stiffness and consequently more stable regions (a larger *z-width*). A new stability analysis was performed to predict the stability boundary of this dual-rate haptic system. The result is a new closed-form equation that relates the physical parameters of the HD to the sampling times, time delay, and the impedance parameters of the VE. Using these equations, the entire stability boundary can be determined without any limitation on sampling times, time delays, or virtual damping. It was shown that these closed-form equations are consistent with prior work in specific cases and have been verified by simulations and experiments.

Simulating virtual mass is a challenging task that can enhance the stability and transparency of the HD. In single-rate haptic systems, this task becomes difficult due to the uncertainties involved in calculating acceleration via backward differencing from velocity. However, using a dual-rate control system can reduce these uncertainties, making the calculation of acceleration via backward differencing of velocity more accurate. Future work will focus on extending the dual-rate control to haptic systems that render virtual mass. Designing dual-rate controllers to improve stability and transparency in dual-rate HDs is an open challenge. Another area for future exploration is extending the results achieved here to multi-DOF haptic systems.

References

[1] N. Yilmaz, B. Burkhart, A. Deguet, P. Kazanzides, and U. Tumerdem, "Sensorless transparency optimized haptic teleoperation on the da vinci research kit," *IEEE Robot. Automat. Lett.*, vol. 9, no. 2, pp. 971–978, Feb. 2024.

[2] X. Li, R. Zhao, X. Chai, Z. Wang, Q. Tong, and W. Ding, "VibroBot: A lightweight and wirelessly programmable vibration bot for haptic guidance," *IEEE Robot. Automat. Lett.*, vol. 9, no. 12, pp. 10882–10889, Dec. 2024.

[3] Y. Liu, R. Leib, and D. W. Franklin, "Follow the force: Haptic communication enhances coordination in physical human-robot interaction when humans are followers," *IEEE Robot. Automat. Lett.*, vol. 8, no. 10, pp. 6459–6466, Oct. 2023.

IEEE Robotics and Automation Letters (RA-L) paper, presented at ICRA 2026, Vienna, Austria. Cite as RA-L paper.

[4] A. Mashayekhi, A. Karami, and B. Siciliano, "A new approach for simplifying multi-degree of freedom haptic device dynamics model," *J. Intell. Robotic Syst.*, vol. 108, no. 1, 2023, Art. no. 4.

[5] A. Karami and A. Mashayekhi, "Improving haptic device stability through redundancy resolution," in *Proc. 10th RSI Int. Conf. Robot. Mechatron. (ICRoM)*, IEEE, 2022, pp. 527–532.

[6] A. Mashayekhi, S. Behbahani, F. Ficuciello, and B. Siciliano, "Delay-dependent stability analysis in haptic rendering," *J. Intell. Robotic Syst.*, vol. 97, pp. 33–45, 2020.

[7] J. J. Gil, A. Avello, A. Rubio, and J. Florez, "Stability analysis of a 1-DOF haptic interface using the Routh-Hurwitz criterion," *IEEE Trans. Control Syst. Technol.*, vol. 12, no. 4, pp. 583–588, Jul. 2004.

[8] J. J. Gil, E. Sánchez, T. Hulin, C. Preusche, and G. Hirzinger, "Stability boundary for haptic rendering: Influence of damping and delay," *J. Comput. Inf. Sci. Eng.*, vol. 9, no. 1, 2009, Art. no. 011005.

[9] T. Hulin, A. Albu-Schäffer, and G. Hirzinger, "Passivity and stability boundaries for haptic systems with time delay," *IEEE Trans. Control Syst. Technol.*, vol. 22, no. 4, pp. 1297–1309, Jul. 2014.

[10] J. E. Colgate and J. M. Brown, "Factors affecting the Z-width of a haptic display," in *Proc. 1994 IEEE Int. Conf. Robot. Automat.*, IEEE, 1994, pp. 3205–3210.

[11] J. J. Gil, A. Ugartemendia, and I. Diaz, "Stability analysis and user perception of haptic rendering combining virtual elastic, viscous and inertial effects," *Appl. Sci.*, vol. 10, no. 24, 2020, Art. no. 8807.

[12] J. J. Gil, A. Ugartemendia, and I. Díaz, "Rendering virtual inertia in haptic interfaces: Analysis and limitations," in *Proc. 2022 Int. Conf. Robot. Automat. (ICRA)*, IEEE, 2022, pp. 8876–8881.

[13] L. Pecly and K. Hashtrudi-Zaad, "Uncoupled stability of kinesthetic haptic systems simulating mass-damper-spring environments with complementary filter," in *Proc. 2022 IEEE/ASME Int. Conf. Adv. Intell. Mechatron. (AIM)*, IEEE, 2022, pp. 97–102.

[14] V. Chawda, O. Celik, and M. K. O'Malley, "Evaluation of velocity estimation methods based on their effect on haptic device performance," *IEEE/ASME Trans. Mechatron.*, vol. 23, no. 2, pp. 604–613, Apr. 2018.

[15] F. Janabi-Sharifi, V. Hayward, and C.-S. Chen, "Discrete-time adaptive windowing for velocity estimation," *IEEE Trans. Control Syst. Technol.*, vol. 8, no. 6, pp. 1003–1009, Nov. 2000.

[16] M. Tomizuka, "Multi-rate control for motion control applications," in *Proc. 8th IEEE Int. Workshop Adv. Motion Control*, IEEE, 2004, pp. 21–29.

[17] M. Koul, S. Khosa, and B. Ahmad, "Elevating haptic interfaces: Dual-rate sampling and field programmable gate array implementation for multi-degree-of-freedom performance enhancement," *Int. J. Mech. Syst. Dyn.*, vol. 4, pp. 171–187, 2024.

[18] M. Minsky, O.-Y. Ming, O. Steele, F. P. Brooks Jr, and M. Behensky, "Feeling and seeing: Issues in force display," in *Proc. 1990 Symp. Interactive 3D Graph.*, 1990, pp. 235–241.

[19] L. Pecly and K. Hashtrudi-Zaad, "General discretization method for enhanced kinesthetic haptic stability," *IEEE Trans. Haptics*, vol. 16, no. 2, pp. 261–275, SecondQuarter 2023.

[20] A. Mashayekhi, S. Behbahani, F. Ficuciello, and B. Siciliano, "Analytical stability criterion in haptic rendering: The role of damping," *IEEE/ASME Trans. Mechatron.*, vol. 23, no. 2, pp. 596–603, Apr. 2018.

[21] K. Lee and D. Y. Lee, "Multirate control of haptic interface for stability and high fidelity," in *Proc. 2004 IEEE Int. Conf. Syst. Man Cybern.*, IEEE, 2004, pp. 2542–2547.

[22] X. Dai, Y. Zhang, Y. Cao, and D. Wang, "Stable multirate control algorithm for haptic dental training system," in *Proc. 1st Int. Conf. Intell. Robot. Appl.*, Wuhan, China, Springer, 2008, pp. 27–35.

[23] A. Weill-Duflos, A. Mohand-Ousaid, S. Haliyo, S. Régnier, and V. Hayward, "Optimizing transparency of haptic device through velocity estimation," in *Proc. 2015 IEEE Int. Conf. Adv. Intell. Mechatron. (AIM)*, IEEE, 2015, pp. 529–534.

[24] M. Koul, M. Manivannan, and S. K. Saha, "Effect of dual-rate sampling on the stability of a haptic interface," *J. Intell. Robotic Syst.*, vol. 91, pp. 479–491, 2018.

[25] S. Ganiny, M. H. Koul, and B. Ahmad, "Stability analysis of a dual-rate haptics controller using discrete-time root-locus method," in *Proc. Machines, Mechanism Robot.*, Springer, 2021, pp. 901–909.

[26] S. Ganiny, M. H. Koul, and B. Ahmad, "Time-delayed dual-rate haptic rendering: Stability analysis and reduced order modeling," *Int. J. Intell. Robot. Appl.*, vol. 5, no. 4, pp. 510–533, 2021.

[27] S. Ganiny, M. H. Koul, and B. Ahmad, "On the determination of stability bounds of time-delayed dual-rate haptics controllers via model order reduction," in *Proc. 5th Int. Conf. Adv. Robot.*, 2021, pp. 1–7.

[28] S. Ganiny, M. H. Koul, and B. Ahmad, "Exact discrete-time stability analysis of multi-DOF haptic rendering: Impact of multi-rate, time-delay, and mechanical parameters," *in Proc. Inst. Mech. Engineers, Part C: J. Mech. Eng. Sci.*, 2024, vol. 238, no. 22, pp. 10816–10835.

[29] A. Mashayekhi, S. Behbahani, F. Ficuciello, and B. Siciliano, "Influence of human operator on stability of haptic rendering: A closed-form equation," *Int. J. Intell. Robot. Appl.*, vol. 4, no. 4, pp. 403–415, 2020.

[30] N. Diolaiti, G. Niemeyer, F. Barbagli, and J. K. Salisbury, "Stability of haptic rendering: Discretization, quantization, time delay, and coulomb effects," *IEEE Trans. Robot.*, vol. 22, no. 2, pp. 256–268, Apr. 2006.

[31] A. Mashayekhi, R. B. Boozarjomehry, A. Nahvi, A. Meghdari, and P. Asgari, "Improved passivity criterion in haptic rendering: Influence of coulomb and viscous friction," *Adv. Robot.*, vol. 28, no. 10, pp. 695–706, 2014.

[32] A. Mashayekhi, A. Nahvi, A. Meghdari, and H. Mohtasham Shad, "A new haptic interaction with a visual tracker: Implementation and stability analysis," *Int. J. Intell. Robot. Appl.*, vol. 5, pp. 37–48, 2021.

[33] H. Choi, N. G. Kim, A. Jafari, H. Singh, and J.-H. Ryu, "Virtual inertia as an energy dissipation element for haptic interfaces," *IEEE Robot. Automat. Lett.*, vol. 7, no. 2, pp. 2708–2715, Apr. 2022.

[34] T. Verstraten, R. Furnémont, P. Lopez-Garcia, D. Rodriguez-Cianca, B. Vanderborght, and D. Lefeber, "Kinematically redundant actuators, a solution for conflicting torque–speed requirements," *Int. J. Robot. Res.*, vol. 38, no. 5, pp. 612–629, 2019.

[35] A. Khorasani et al., "Mitigating collision forces and improving response performance in human-robot interaction by using dual-motor actuators," *IEEE Robot. Automat. Lett.*, vol. 9, no. 6, pp. 5982–5989, Jun. 2024.

[36] A. Mashayekhi, M. Mashayekhi, and B. Siciliano, "Identification and optimization of the operator's hand and a haptic device dynamic, using artificial intelligence methods," *Int. J. Dyn. Control*, vol. 11, no. 6, pp. 3052–3061, 2023.